

## Density of reef sharks estimated by applying an agent-based model to video surveys

Mathew A. Vanderklift<sup>1,\*</sup>, Fabio Boschetti<sup>1</sup>, Clovis Roubertie<sup>1</sup>, Richard D. Pillans<sup>2</sup>, Michael D. E. Haywood<sup>2</sup>, Russell C. Babcock<sup>2</sup>

<sup>1</sup>CSIRO Wealth from Oceans Flagship, Private Bag 5, Wembley, Western Australia 6913, Australia

<sup>2</sup>CSIRO Wealth from Oceans Flagship, 41 Boggo Rd, Dutton Park, Queensland 4102, Australia

\*Corresponding author: mat.vanderklift@csiro.au

*Marine Ecology Progress Series 508: 201–209 (2014)*

---

**Supplement.** Description of analyses conducted to investigate sensitivity to parameter uncertainty

### INFLUENCE OF CHOICE OF MINIMUM AND MAXIMUM STEP LENGTHS

As described in the main text, Eq. (2) gives the probability of occurrence of a step of a given length  $r$ . To test the extent to which the outcomes of a model were influenced by the choice of  $minstep$  and  $maxstep$  we followed this approach:

- we created a simplified model domain with a spatial orientation similar to the study area (Fig. S1a),
- we let  $minstep$  range from 1 to 6 m and  $maxstep$  from 80 to 120 m,
- for each combination of  $minstep$  and  $maxstep$  we performed 100 runs within the model domain, using a density of 50 ind. km<sup>-2</sup>, with shark speed = 0.7 m and  $\mu = 1.7$ ,
- for each model run we calculated the value of  $F_{obs}$  producing a set of 100  $F_{obs}$  values for each [ $minstep$ ,  $maxstep$ ] pair, which we called  $F_{obs} Set$ ,
- we defined MinS = 3 m and MaxS = 100 m, the  $minstep$  and  $maxstep$  used in this work, respectively, and
- for each combination of  $minstep$  and  $maxstep$ , we used the Kolmogorov–Smirnov test to test the null hypothesis that  $F_{obs}Set(minstep, maxstep)$  and  $F_{obs}Set(MinS, MaxS)$  belong to the same distribution.

The Kolmogorov–Smirnov test indicated there was no statistically significant difference in  $F_{obs}$  for all [ $minstep$ ,  $maxstep$ ] pairs ( $p > 0.05$ ). Fig. S1b shows the mean of  $F_{obs} Set(minstep, maxstep)$  for each [ $minstep$ ,  $maxstep$ ] pair. No obvious structure can be detected in the image, nor any trend related to increasing  $minstep$  and  $maxstep$ . We therefore infer that, within the ranges we analysed, the choice of  $minstep$  and  $maxstep$  used in this study did not have any noticeable effect on the results presented in the main text.

## INFLUENCE OF CAMERA DENSITY AND LOCATION

The uncertainty in estimates of density depends on the density of cameras (i.e. the number of cameras per unit area), the positioning of the cameras and the length of the camera recording. Increasing the density of cameras would provide more reliable estimates of the frequency of observation, but this would be non-linear, so that the relationship between the distance between cameras and shark movement is such that further increases in camera density provide diminished returns in terms of accuracy (Figs. S2 & S3). The range between the 10th and 90th percentiles is reduced as camera density increases (Fig. S2), demonstrating that increasing camera density (e.g. from 0.3 to 2.9 cameras  $\text{km}^{-2}$ ) increases the accuracy of the estimates of shark density.

A considerable improvement in accuracy is attained between 0.3 to 1 cameras  $\text{km}^{-2}$ , while further increases in camera density provide diminished returns in terms of accuracy. This result should be considered problem dependent, and not a general rule, as it specifically applies to the configuration of habitats and camera locations used in our study. However, it demonstrates how the approach could be used to design a field survey.

For low shark densities (e.g.  $<1.5$  sharks  $\text{km}^{-2}$ ), estimates yielded by low camera densities become unreliable (Fig. S2); the 90th percentiles for different camera densities intersect at low shark densities; 90th percentiles converge towards infinity and the 10th percentile shows non-monotonic behaviour. This pattern provides some indication of the minimum density of cameras, as a function of the expected population size, which should be used in order to obtain results of sufficient reliability. In our case, for example, we should not expect the use of a camera density  $<0.25$  cameras  $\text{km}^{-2}$  to give reliable estimates of density when the true density is  $<1.5$  sharks  $\text{km}^{-2}$ .

The location of the camera also will affect the probability of an observation. Ideally, cameras should be positioned in such a way to increase the probability of shark detection, and doing so may require accounting for bathymetry and habitat. Fig. S4 (obtained by modeling 500 individuals) illustrates this, showing an example of the how movement around obstacles could influence the spatial distribution of individuals. In situations in which unoriented movement (e.g. Brownian motion,  $k_{\text{dir}} = 0$ ), results in roughly similar visitation on both sides of a reef, the location of the cameras is likely to have relatively little influence on the frequency of observation (bottom left panel). The bottom right panel shows an alternative situation, in which individuals follow Lévy flight, with directional movement towards a foraging area at the right hand side ( $k_{\text{dir}} = 0.25$ ). In order to reach the foraging area, individuals need to move around the obstacles (e.g. reefs), which results in high visitation left of the obstacles; once they get around the obstacles, they can proceed directly to the foraging area, resulting in low visitation immediately to the right of the obstacles. Locating the cameras in different areas would result in different frequencies of detection and, consequently, high uncertainty concerning the estimates of shark abundance.

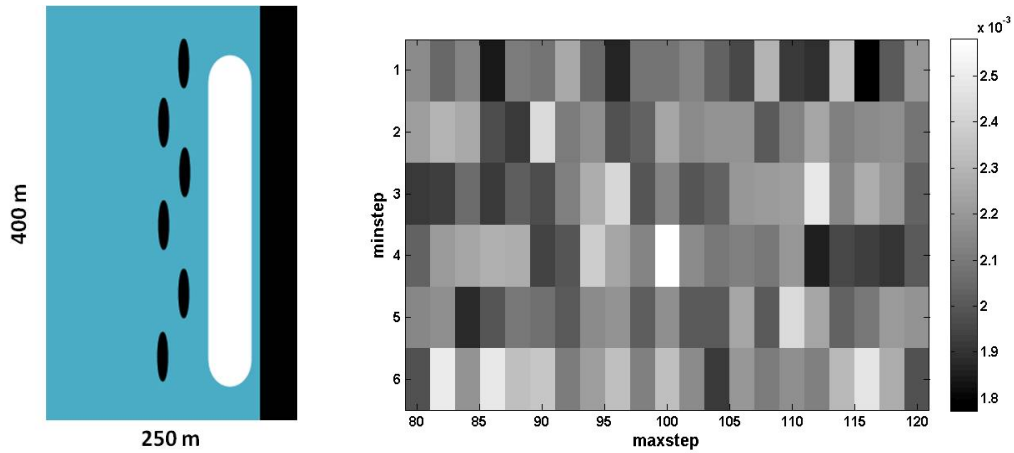


Fig. S1. Results of testing to determine the potential influence of the choice of step length. (a) Simplified model domain used for sensitivity analysis of the impact of minimum and maximum step length in the Lévy Walk. (b) Mean  $F_{\text{obs}}^{\text{Set}}$  for each  $[\text{minstep}, \text{maxstep}]$  pair

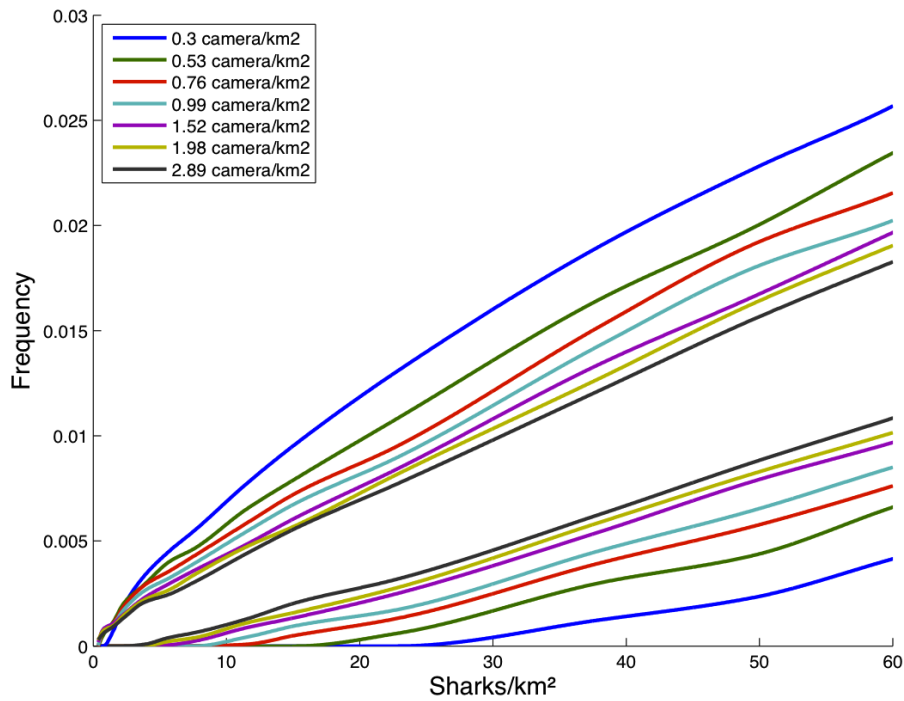


Fig. S2. Modelled frequency of observations  $F_{\text{mod}}^s$  plotted against shark densities for different camera densities, for  $k_{\text{dir}} = 0$ . The 10th and 90th percentiles of the distributions for each camera density are shown. Colours refer to camera densities, ranging from 0.3 to 2.9 cameras  $\text{km}^{-2}$

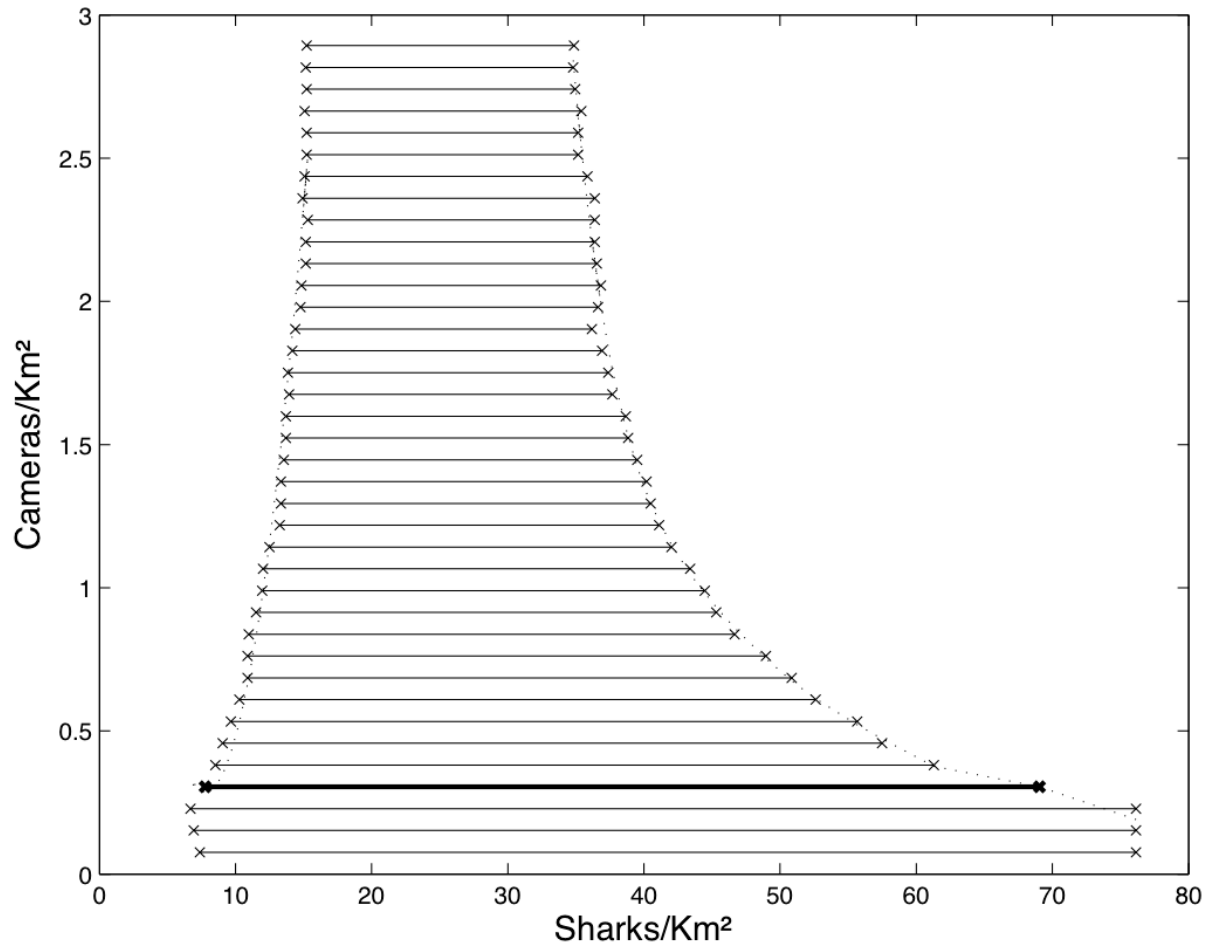


Fig. S3. Camera density plotted against shark density  $k_{\text{dir}} = 0$ . Plot shows the range between the 10th and 90th percentiles. Thick black line represents the densities of cameras used in our study ( $0.3 \text{ cameras km}^{-2}$ )

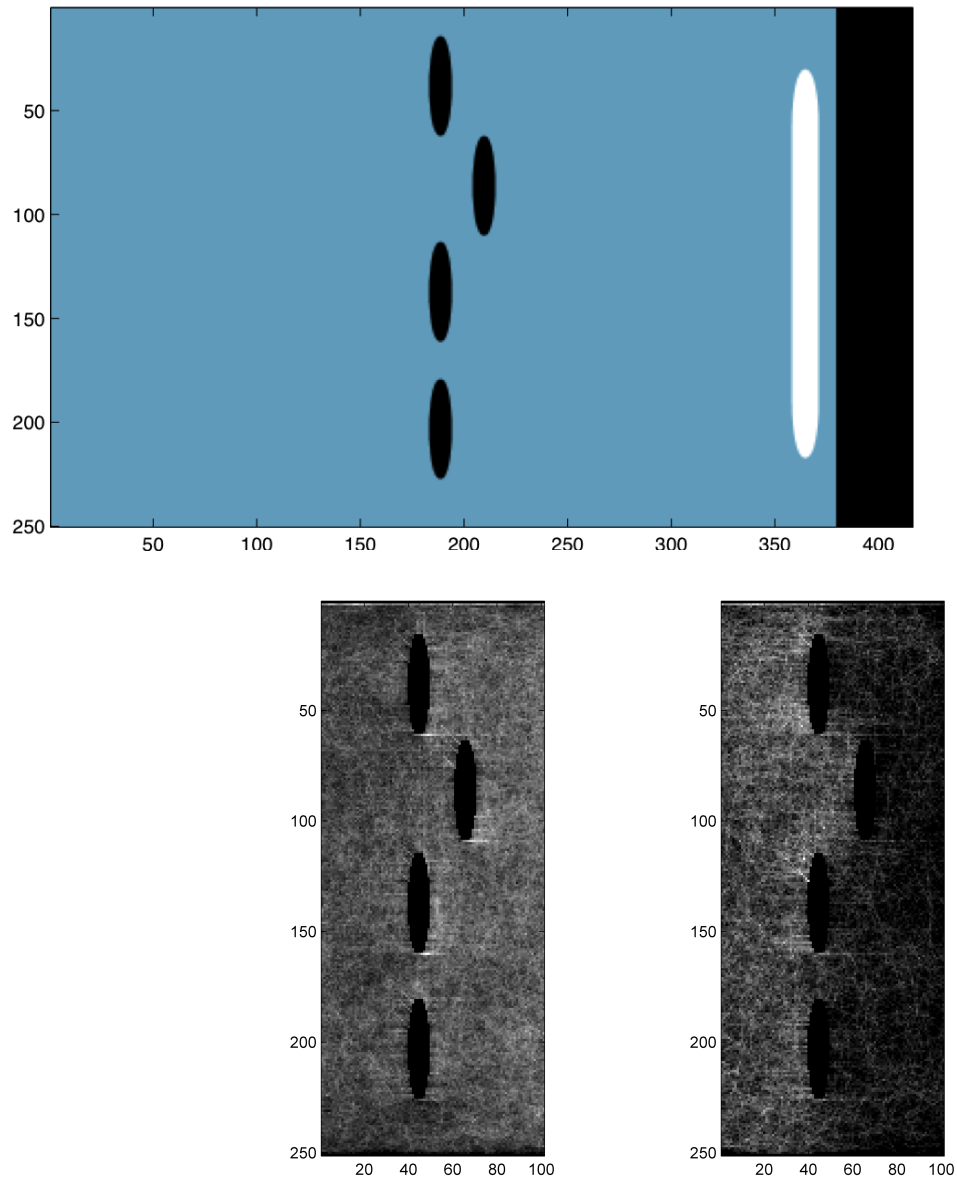


Fig. S4. An example of the impact of how movement patterns can influence spatial distribution, and, therefore, the probability of detection, obtained by modelling movement for 500 individuals. Upper panel: a simplified model domain. Black areas represent obstacles (e.g. coast and reefs); the white area represents a foraging area. Lower left panel: the result of simulations with unoriented movement ( $k_{\text{dir}} = 0$ ); lower right panel: the result of simulations with oriented movement ( $k_{\text{dir}} = 0.25$ ); shading shows the number of times individuals cross each pixel (dark = high visitation)